



THE UNIVERSITY *of* EDINBURGH

Edinburgh Research Explorer

Coherence properties of liquid crystal lasers

Citation for published version:

Hansford, D, Payne, A, Wilkinson, T, Hands, P & Morris, S 2015, 'Coherence properties of liquid crystal lasers', European Conference on Liquid Crystals (ECLC), Manchester, United Kingdom, 7/09/15 - 11/09/15.

Link:

[Link to publication record in Edinburgh Research Explorer](#)

Document Version:

Peer reviewed version

General rights

Copyright for the publications made accessible via the Edinburgh Research Explorer is retained by the author(s) and / or other copyright owners and it is a condition of accessing these publications that users recognise and abide by the legal requirements associated with these rights.

Take down policy

The University of Edinburgh has made every reasonable effort to ensure that Edinburgh Research Explorer content complies with UK legislation. If you believe that the public display of this file breaches copyright please contact openaccess@ed.ac.uk providing details, and we will remove access to the work immediately and investigate your claim.



Coherence properties of Liquid Crystal Lasers

David J Hansford¹, Andrew Payne², Timothy D Wilkinson², Philip J W Hands³, Stephen M Morris¹

1. Department of Engineering Science, University of Oxford, Parks Road, Oxford, OX1 3PJ, UK
2. Department of Engineering, University of Cambridge, 9 JJ Thomson Avenue, Cambridge, CB3 0FA, UK
3. Department of Engineering, University of Edinburgh, Colin Maclaurin Road, Edinburgh, EH9 3DW, UK

1. Introduction



Figure 1. Four different light sources are used in this poster, a continuous wave narrow linewidth laser (He-Ne, JDS Uniphase), a pulsed solid-state laser (Nd:YAG, CryLas), a pulsed Liquid Crystal Laser (LCL) and a broadband LED (Thorlabs).

Recently, many novel light sources have been developed that produce light with interesting characteristics. It is important to measure these characteristics in order to fully understand these sources and their potential uses. The coherence of a light source is of paramount interest as it determines the light's ability to interfere with itself for uses such as holographic projection. This poster describes two complimentary techniques used to measure the temporal and spatial coherence of a range of pulsed or continuous-wave lasers.

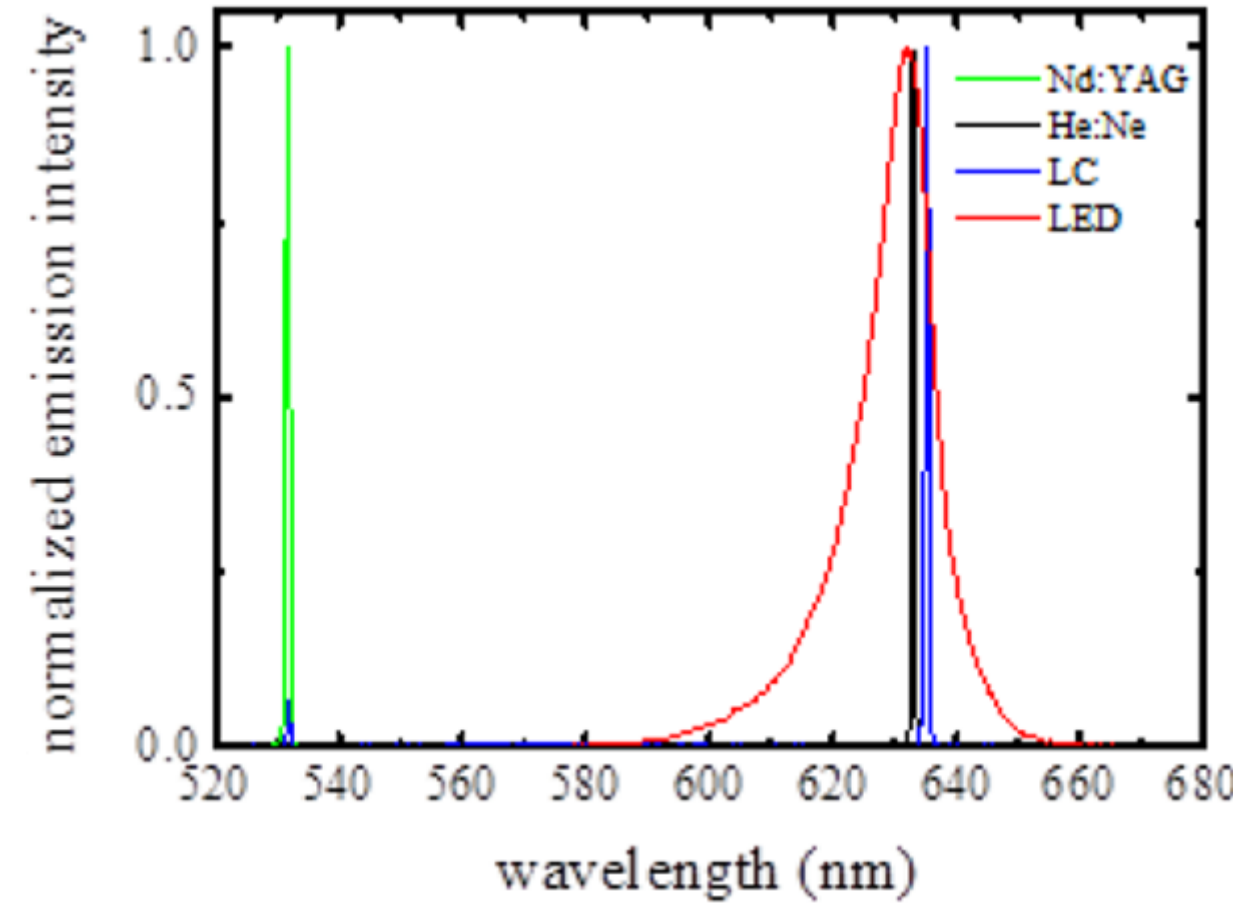


Figure 2. Emission spectra of the four light sources in this study: each spectrum is normalised to the peak intensity of that source

2. Coherence

Temporal coherence is the measure of phase correlation between two parts of a beam separated only in time. A first order approximation can be found from the linewidth of a source as such:

$$l_c \sim \frac{\lambda_0^2}{\Delta\lambda}$$

It can also be measured through observation of interference between a beam of light and a time delayed version of itself, such as in a Michelson Interferometer¹.

Spatial coherence is the measure of phase correlation between two points transverse to the propagation direction, thus showing how uniform the phase of a wave front is. It can be measured with Young's double slit experiment¹, one slit separation at a time.

The techniques described in this poster can measure the entire temporal and spatial coherence functions of a pulsed laser in a single pulse.

Holographic projection uses the interference of light to reproduce a desired image in the replay field. This requires good temporal coherence, but high spatial coherence leads to speckle. Some novel lasers, such as LCLs, appear to offer a combination of high temporal and low spatial coherence making them ideal for such applications.

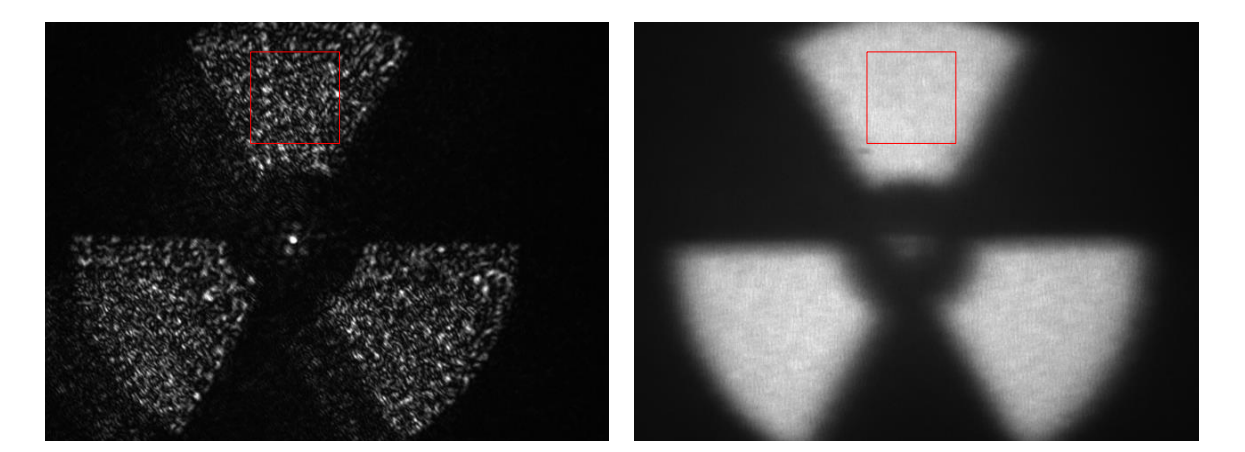
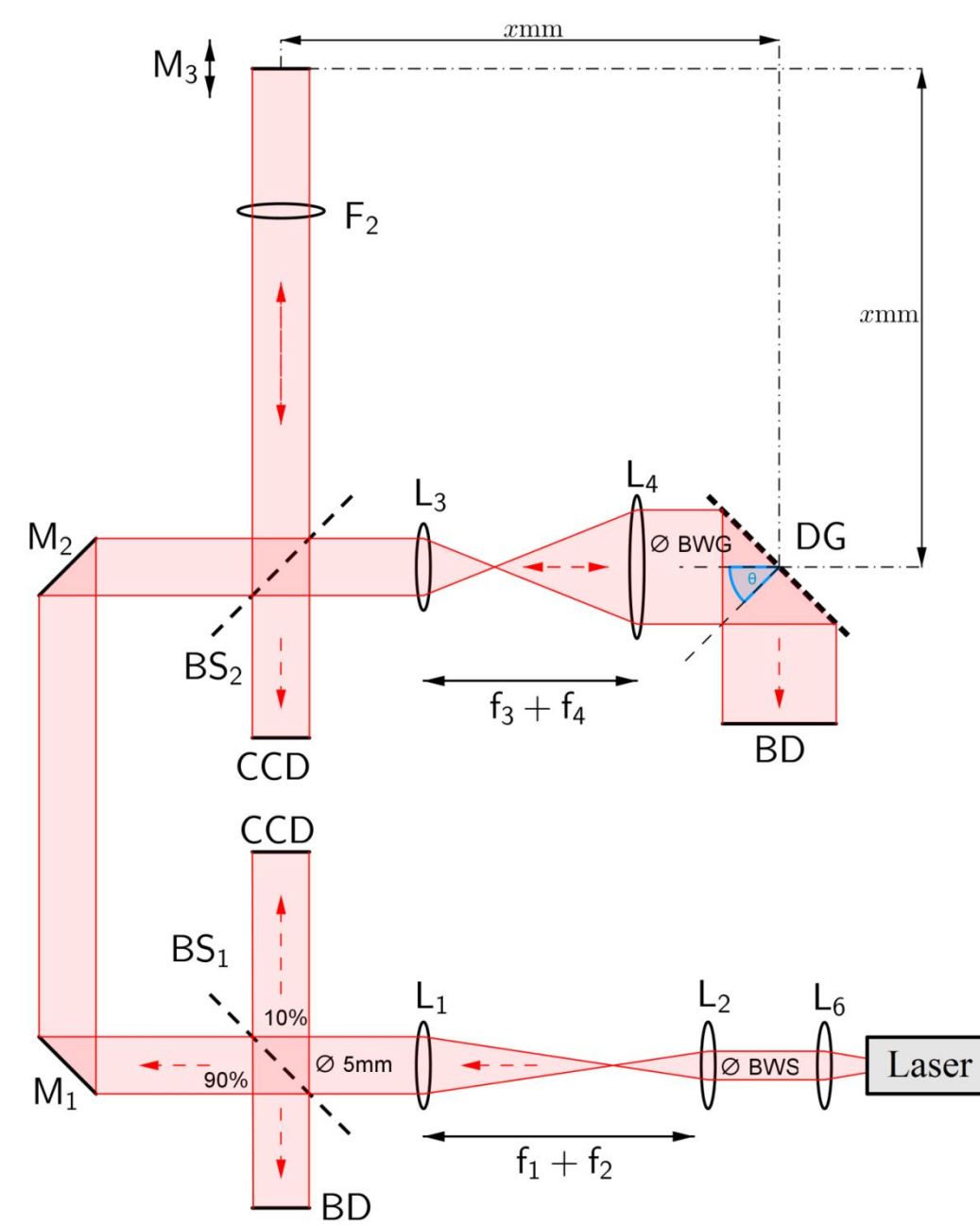


Figure 3. Speckle artefacts visible in He-Ne holographic projection

3. Temporal Coherence

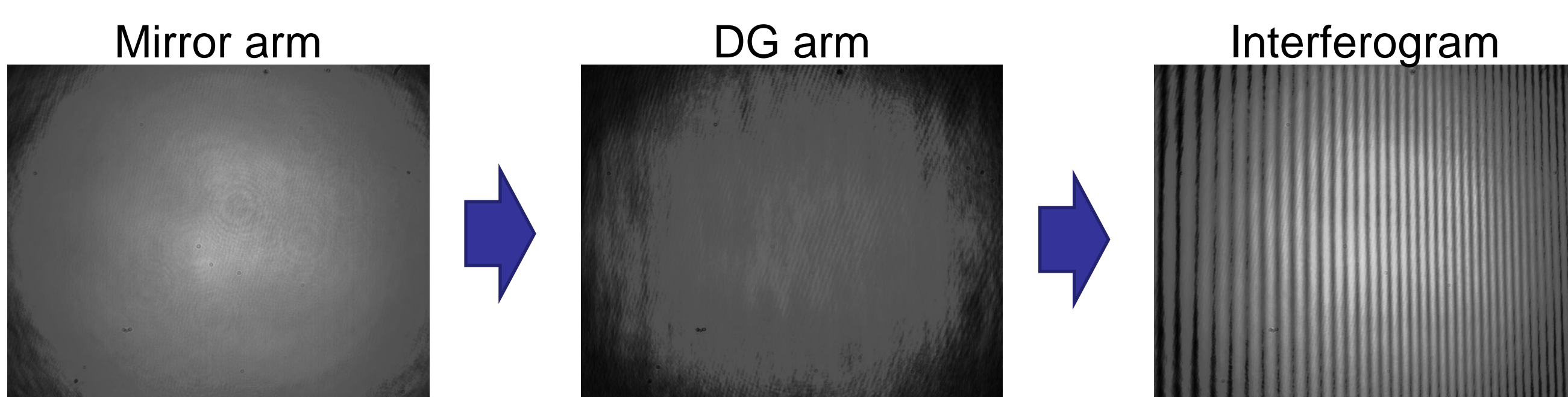


The mirror from one arm of a standard Michelson Interferometer is replaced by a blazed Diffraction Grating (DG) in a Littrow mount². This reflects light with optical path that varies across the beam by up to 43.6mm, allowing the a temporal coherence function over this distance to be measured in a single pulse.

Coherence is measured through visibility of fringes in interferogram.

Figure 4 (left). Michelson Interferometer with DG in place of one mirror

Figure 5 (below). Beam profile reflected from mirror (1) and Blazed Diffraction Grating (2), interferogram of combined beams (3). Produced using He-Ne laser.



4. Spatial Coherence

A non-redundant array (NRA) of nine apertures samples the expanded beam front at range of separations simultaneously. The FT of the captured interferogram is combined with the intensity profile of the beam to produce a two-dimensional coherence surface from a single pulse³.

$$|\gamma_{12}| = \frac{|c_{12}| \sqrt{I_N}}{|c_0| \sqrt{I_1 I_2}}$$

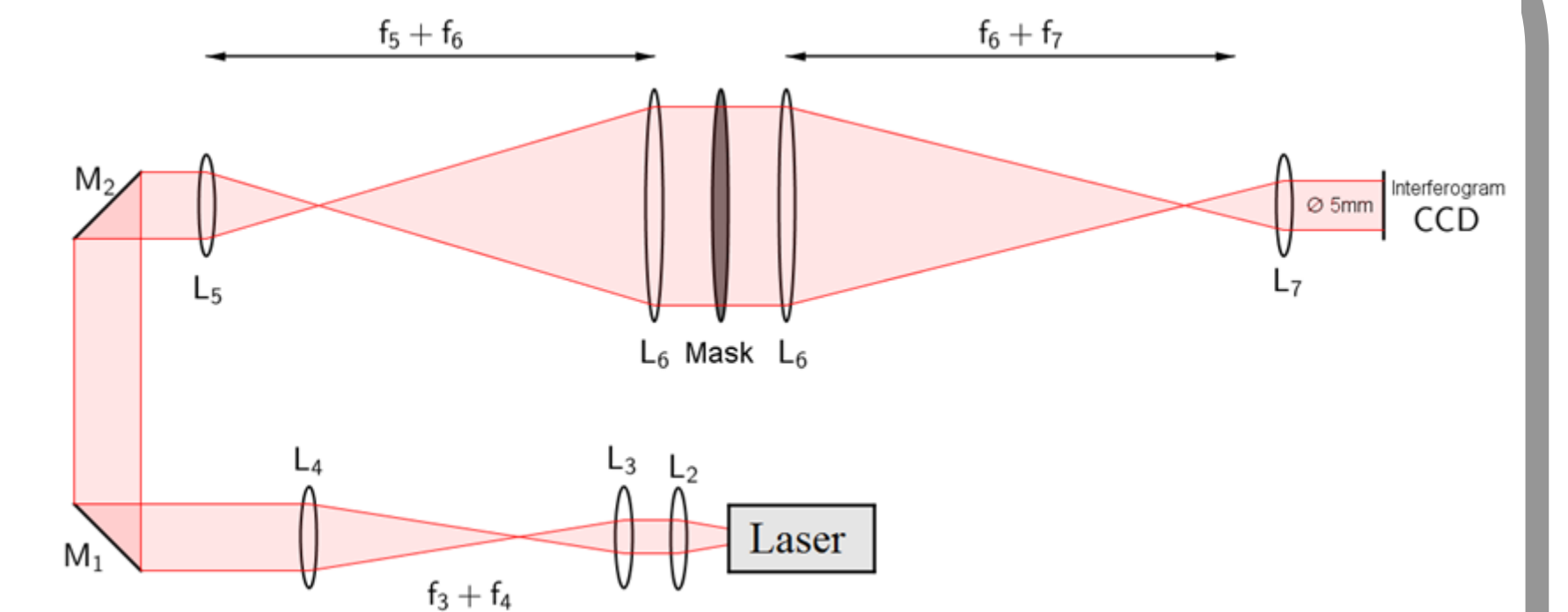
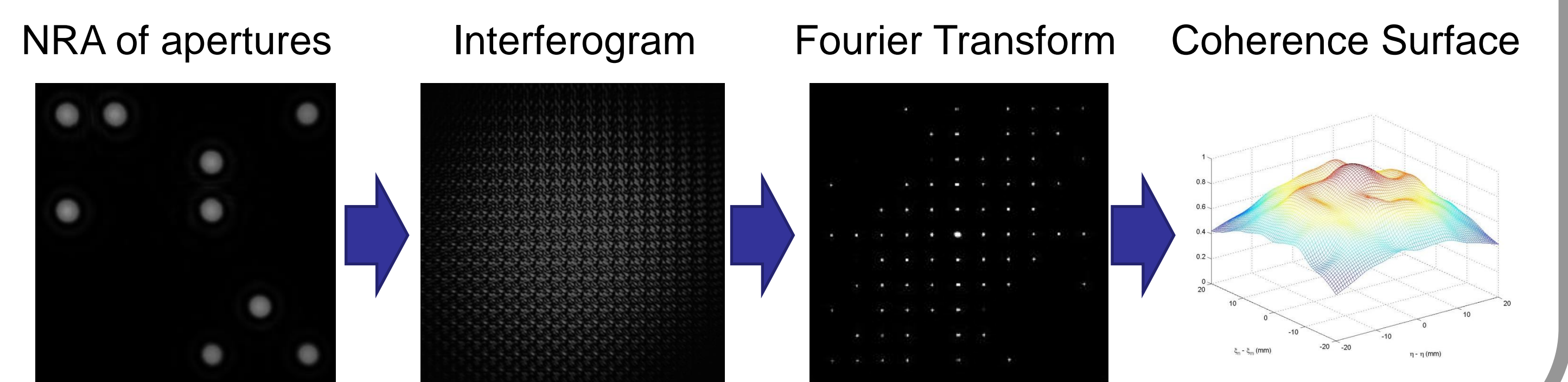


Figure 6 (above). Spatial coherence measurement using NRA mask and achromatic doublet beam expanding lenses.

Figure 7 (below). (1) Design of mask (2) Interferogram formed at CCD (3) Fourier Transform (4) 2D Coherence Surface. Produced using He-Ne Laser



5. Visibility

Three lasers tested using Young's Double Aperture experiment for a range of separations. Intensity differences at each aperture are accounted for with the following mutual coherence equation:

$$|\gamma_{12}| = \frac{I_{max} - I_{min}}{I_{max} + I_{min}} \times \frac{I_{left} + I_{right}}{2 \sqrt{I_{left}} \sqrt{I_{right}}}$$

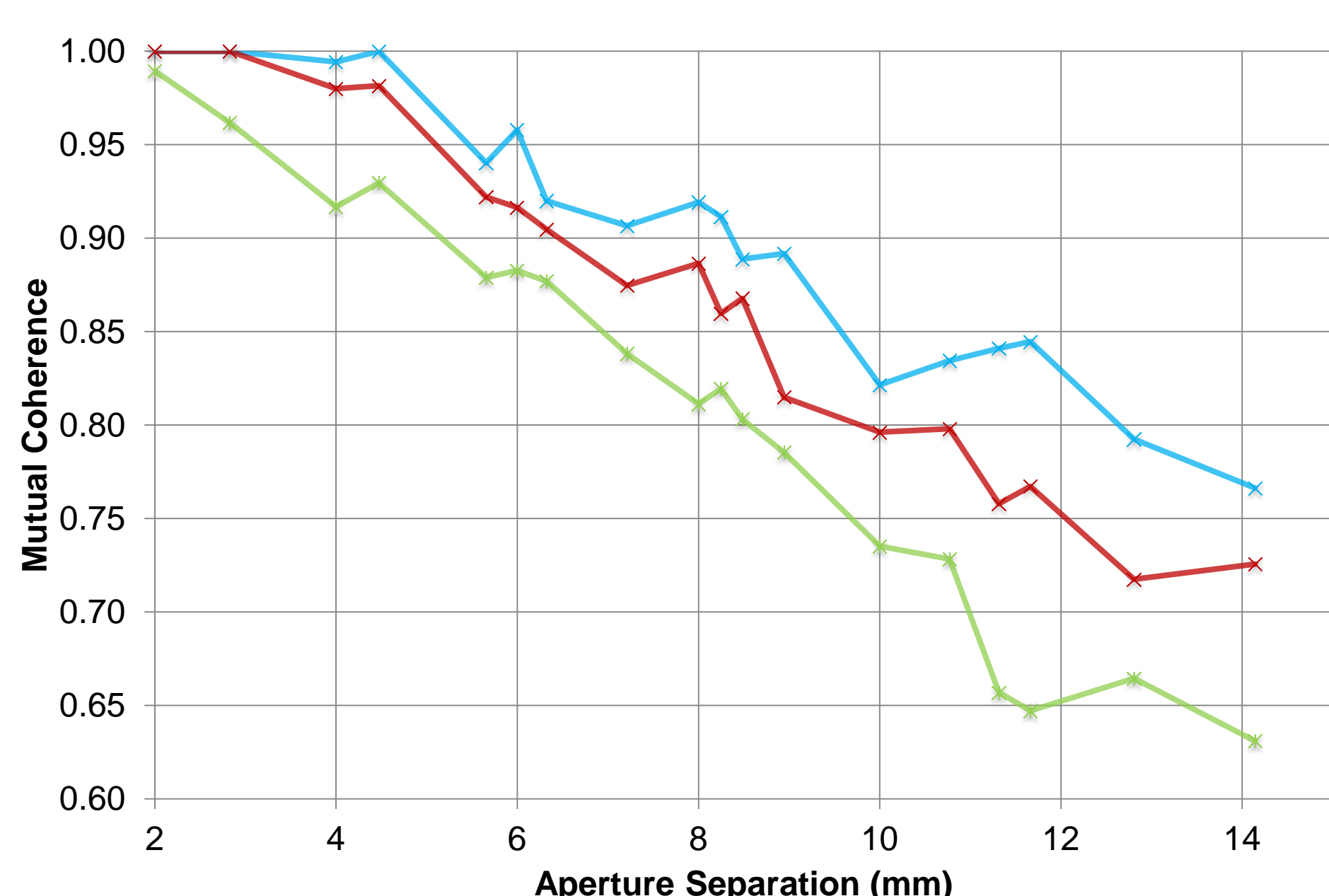


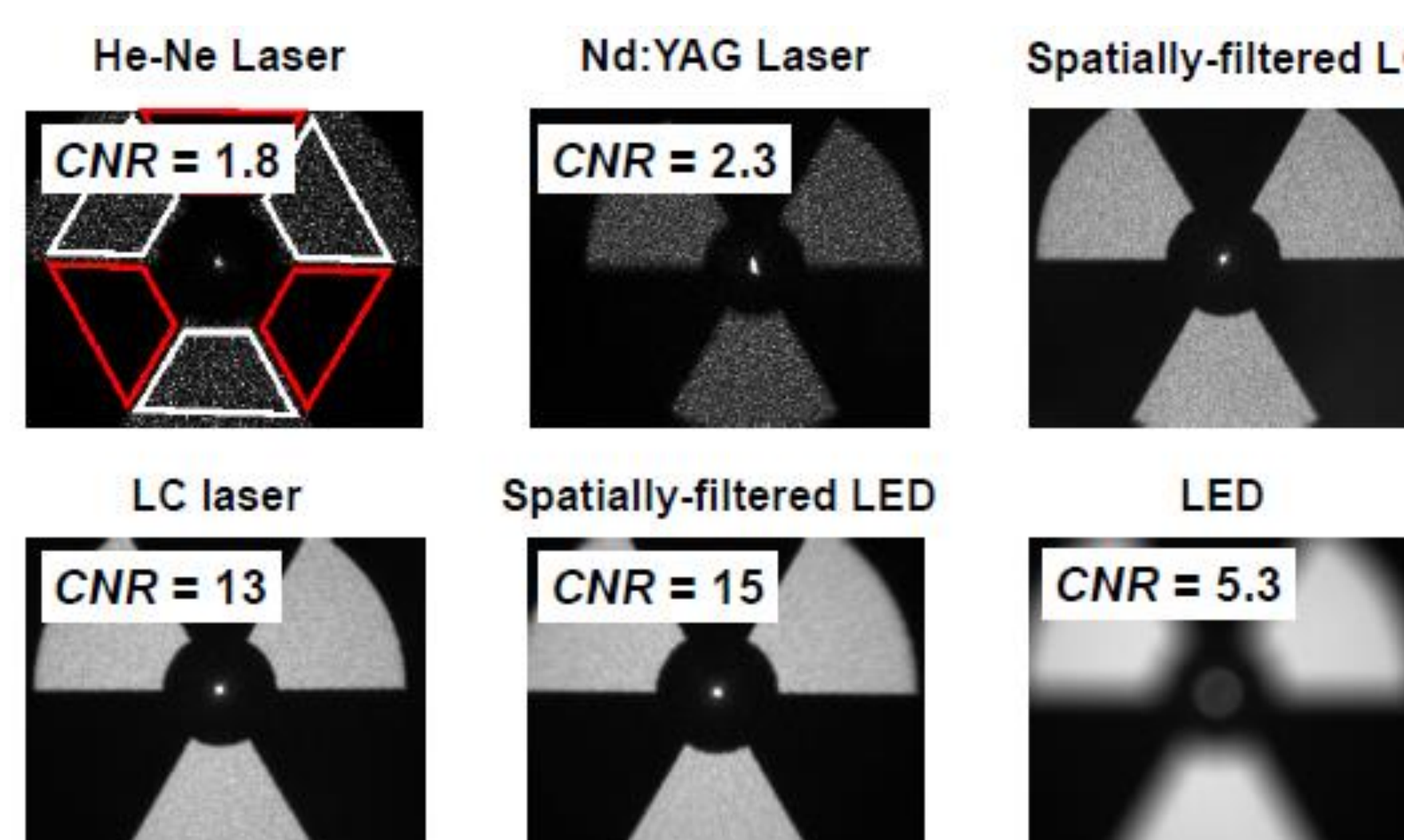
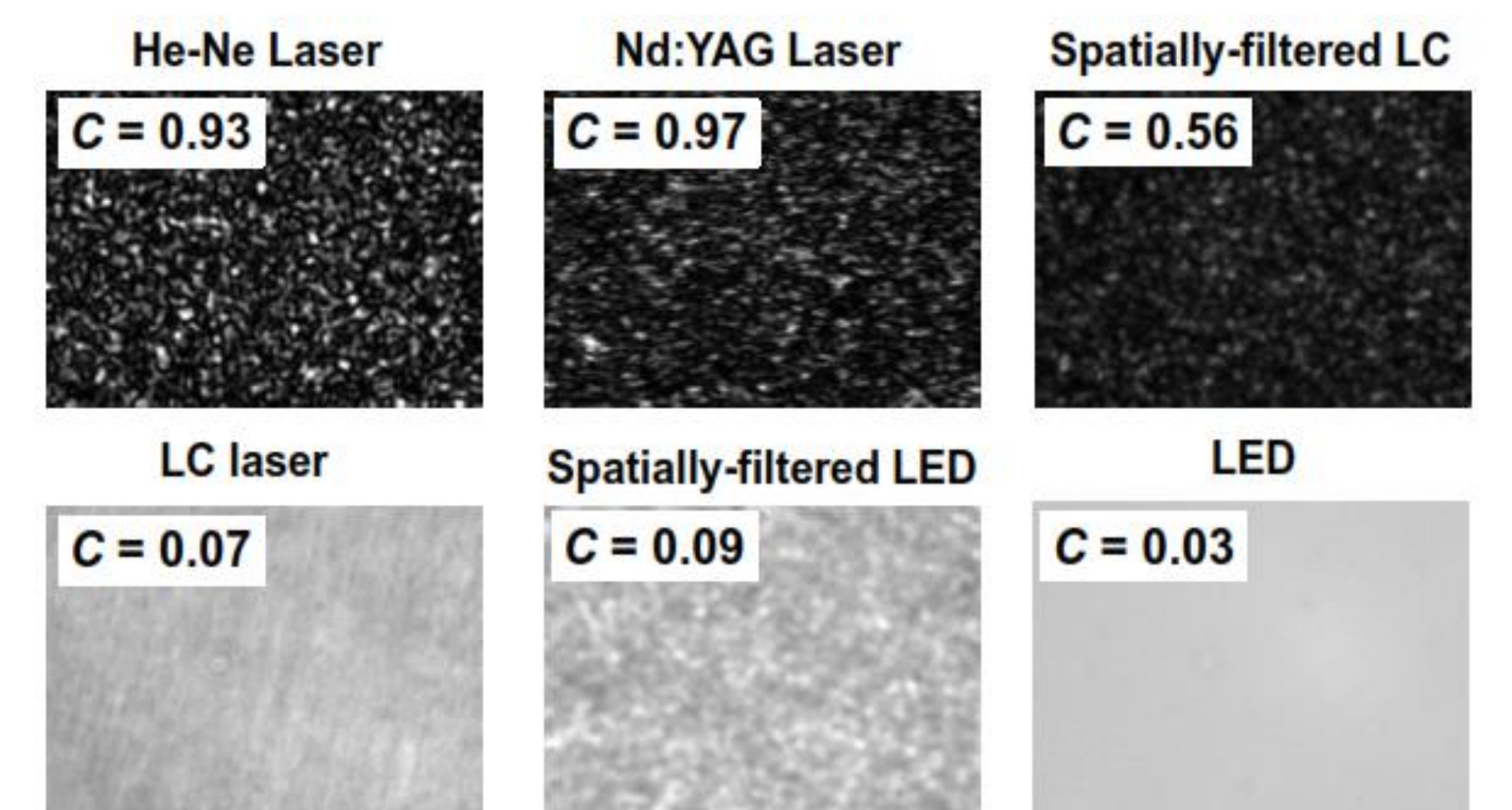
Figure 8. Graph showing mutual coherence measured by visibility of interference fringes in Young's double aperture set-up with a range of aperture separations. (Blue) He-Ne 15mW (Red) He-Ne 10mW (Green) Nd:YAG. Beam expansion: 41.7x

6. Liquid Crystal Lasers

Figure 9. Greyscale images of speckle captured on a CCD camera created by the introduction of a diffuser.

$$C = \frac{\sigma_I}{\langle I \rangle} = \frac{\sqrt{\langle I^2 \rangle - \langle I \rangle^2}}{\langle I \rangle}$$

The speckle contrast C varies from 0, for an incoherent source, to 1 for a fully coherent source.



Contrast to noise ratio (CNR):

$$CNR = \frac{\langle I_f \rangle - \langle I_b \rangle}{(\sigma_f - \sigma_b)/2}$$

Figure 10. Reconstructed images from a multi-level phase hologram captured in the replay field for the different light sources. The foreground regions used in the above equation are shown in white on the He-Ne image, the background are shown in red.